Effect of Cathode Contacting on Anode Supported Cell Performances and Degradation

R. Spotorno[a], P. Piccardo[a], G. Schiller[b]

[a] Department of Chemistry and Industrial Chemistry, University of Genoa, Genoa, Italy
[b] German Aerospace Center (DLR), Stuttgart, Germany

The contact geometry effect on anode-supported cells (ASC) has been evaluated comparing the use of platinum meshes and Crofer 22 APU bipolar plates as current collectors. Additionally, the application of a $La_{0.6}Sr_{0.4}Co_{0.2}Fe_{0.8}O_3$ (LSCF) paste between the electrode and the current collector allowed to estimate the beneficial effect of the contacting layer enhancing the current distribution at the cathode side. Cells have been electrically loaded for 100 hours to investigate the polarization effects on their performances by means of current-voltage curves and electrochemical impedance spectroscopy. Post-experiment analyses have been carried out to support the electrochemical observations.

Introduction

Stacking Solid Oxide Fuel Cells implies the use of contacting layers, especially in the cathode compartments where ohmic losses are introduced at the interface between the electrode and the interconnect due to the high interfacial resistance and the lowered contact area caused by geometrical and porosity issues (1). Such losses affect the current distribution over the electrodes strongly influencing the system performances in terms of power outputs. Whereas the cell polarization losses are dependent on the current load on the cell (2), the contacting issues are weakly influenced by the operating conditions, implying the need to solve them at the structural level in order to ensure high stack performances (2, 3). The application of a contacting layer between the cathode and current collector (i.e. platinum mesh or steel bipolar plate) enhances the electrical contact and improves the planar conductivity over the cathode area (4).

For understanding the effect of the contacting geometry, the application of a contacting paste is important not only to mitigate the losses in a power system but also for the cell characterization since the current distribution can significantly influence the results of the electrochemical analyses. In this study a dedicated testing setup has been used to test anode-supported cells with different contacting solutions. The performances of such system have been investigated by means of current-voltage curves. Electrochemical impedance spectroscopy measurements were carried out to distinguish the loss contributions within the system and to study the degradation phenomena. Scanning electron microscopy equipped with energy dispersive X-ray spectroscopy and X-ray diffraction techniques were adopted as post-experiment characterization methods to investigate microstructural changes and elements migration in order to confirm the observed changes in performances.

Materials and methods

In this study commercially available anode-supported cells (ASC) manufactured by CeramTec AG were tested. Such cells consisted of a 50 mm x 50 mm Ni/8YSZ-cermet anode (where 8YSZ: 8 mol% Y_2O_3 doped ZrO_2), an 8YSZ electrolyte with GDC ($Ce_{0.8}Gd_{0.2}O_{2-\delta}$) interlayer at the cathode side followed by a LSCF ($La_{0.6}Sr_{0.4}Co_{0.2}Fe_{0.8}O_{3-\delta}$) 40 mm x 40 mm cathode (figure 1).

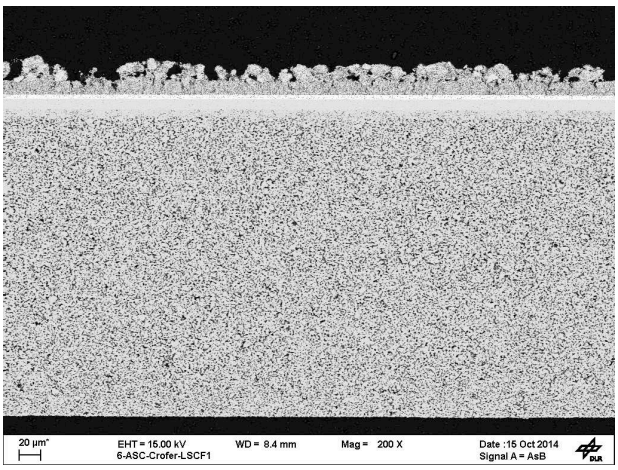

Figure 1. SEM-BSE image of an ASC cross-section.

The preparation of the contacting paste to be applied on the cathode side consisted of commercially available LSCF (FCM, USA) mixed with a solvent blend (94 wt.% terpineol, 6 wt.% polyethylene glycol) to form an ink (60 wt.% powder, 40 wt.% solvent). Such mixture has been homogenised in a Exakt 80E three roll mill (Exakt Advanced Technologies GmbH, Germany). LSCF ink has been brushed on ASC obtaining a homogeneous layer on top of the cathode. The metal current collectors (platinum mesh or bipolar plate) have been applied on the cell right after the paste deposition. Bipolar plates have been produced from Crofer 22 APU (ThyssenKrupp VD) sheets by a stamping process (Graebner Maschinentechnik GmbH & Co. KG, Germany) using a design optimized for testing with ASCs.

Testing of interconnect and contacting solutions effects on cell performances in working conditions have been performed using a dedicated sample holder designed on purpose and reproduced from Macor® (SiO_2 46 wt.%, MgO 17 wt.%, Al_2O_3 16 wt.%, K_2O 10 wt.%, B_2O_3 7 wt.%, F 4 wt.%) (figure 2). It can host an anode-supported cell and it is optimized to achieve a proper gas feeding and distribution at the electrodes.

The electrical contact between the cell and the electronic characterization devices is obtained using platinum meshes at both anode and cathode side. On both sides two meshes have been used, a fine one in direct contact with the electrode and a coarser one spot-welded with the platinum wires used as potential probes and current carriers. At the anode side a fine nickel mesh has been placed between the platinum and the anodic cermet. Such additional mesh is intended to avoid alloying between the platinum contacts and the nickel contained in the anode (5).

An additional part, designed to host a 30 mm x 30 mm metallic bipolar plate, has been developed to reproduce the contact electrode-interconnect in order to test their interaction and the behaviour of the cell with different contacting solutions. Also in this case the electrical wiring is spot-welded to a coarse platinum mesh, which is contacted

with the back side of the bipolar plate. A modification of the gas distributor geometry allowed to force the gas flow through the interconnect channels limiting leakages.

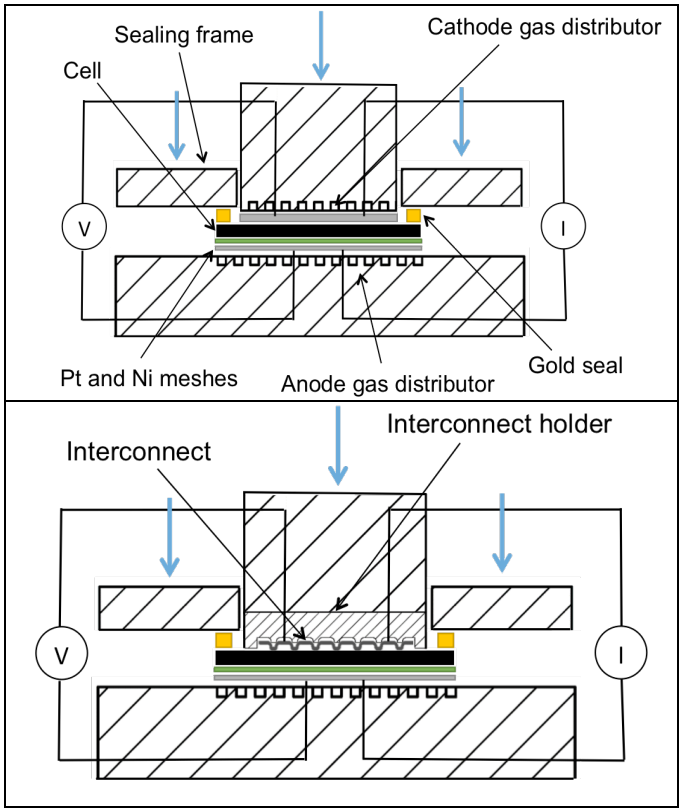

Figure 2. Scheme of testing setup with ceramic gas distributors (above) and with metallic bipolar plate as gas distributor/current collector on the cathode side (below).

Weights (arrows in figure 2) are placed on top of the cell housing to enhance the electrical contacting and the sealing between the two gas compartments, which is achieved using a gold gasket. In this study, 1500 g have been applied on the cathode head obtaining a mechanical load of 9200 Pa on the contacted cathode area. 1400 g were placed on the sealing frame, which compress the gold gasket ensuring gas tightness between the cathode and the anode compartment. Such sealing method has been implemented in order to avoid the use of glass sealants giving the advantages of better experiment reproducibility and ease to set up.

The cell housing is mounted in a furnace capable to heat up to 1000°C and provided with gas and wiring ducts .

Thermocouples have been located in the furnace environment and in the cell housing using proper grooves and thus allowing to monitor the cell temperatures in specific parts (i.e. cathode side, anode side, fuel inlet/outlet, oxidant inlet/outlet) to detect possible combustion of the fuel due to unwanted leakages through the sealant or ceramic components.

Each cell has been heated to 900°C under a dry air flow at the cathode side (0.5 Nl min^{-1}) and dry nitrogen at the anode side (500 Nl min^{-1}). The heating speed was 5°C min^{-1} to avoid excessive thermal shocks of the cell and the ceramic cell housing. At 900°C the reduction of the anode was performed through step-wise increase of the hydrogen concentration in the anode gas flow (6, 7). The gas feeding to the electrodes was turned

in five steps to 1 Nl min^{-1} of 3% wet hydrogen at the anode and 1 Nl min^{-1} of air at the cathode resulting in negligible fuel utilization during the whole testing procedure.

Cells have been electrically loaded for 100 hours bringing their potential to the initial value of 0.9 V applying a fixed current load in galvanostatic mode. The degradation effect on performances was evaluated by monitoring the cell potential decrease during loading, then by polarization curves and electrochemical impedance spectroscopy (EIS) measurements. The electrical characterization has been carried out using an Electrochemical Workstation IM6 (Zahner-Elektrik GmbH & Co. KG, Germany) in a frequency range of 0.1 Hz-100 kHz.

After each test, the cell and bipolar plate were divided and individually studied. XRD analyses were performed on the cell surface using a D8 Discover GADDS X-ray diffractometer (Bruker, Germany), equipped with a VÅNTEC-2000 area detector to investigate the phase composition. Afterwards, cross-sections of samples have been prepared by mounting in epoxy resin, cutting and polishing with a diamond suspension up to 250 nm grain size. Such sections have been observed and analysed using a scanning electron microscope (SEM) Zeiss Evo 40, equipped with EDX detector PentaFET.

Results and discussion

The I-V curves of the cells measured at 750°C highlight the strong influence of the contacting solution on the investigated system performances (figure 3). The cell which was electrically contacted at the cathode side only with a platinum mesh in direct contact with the electrode showed a power density of 423 $mWcm^{-2}$ at 0.7 V and a maximum power density of 480 $mWcm^{-2}$ measured at 0.6 V. Such values are by 30% lower compared to other state-of-the-art cells measured by other authors (6, 7) but comparable with results related to the same type of cells in stacks (8). The use of a shaped bipolar plate as cathodic current collector dramatically decreased the cell performances measuring a power density of 124 $mWcm^{-2}$ at 0.7 V and 136 $mWcm^{-2}$ at 0.6 V. The fast voltage drop observed in this case has been mainly caused by an excessive ohmic contribution as can be seen by the change in the slope of the voltage curve and confirmed by the impedance spectra (figure 4). The ohmic losses due to both contacting issues and the electrolyte resistance are identified as the value of the high-frequency intercept of the AC impedance spectra with the real part axis. For the cell contacted with the Crofer 22 APU bipolar plate an ohmic contribution of 1.542 Ωcm^2, has been measured, more than four times higher compared to the cell contacted by platinum meshes (0.374 Ωcm^2). Such difference is caused by the minimization of the contact points between the metal and the electrode in the case of the bipolar plate. Consequently, also the cell polarization suffered a performance decrease with the worsening of the total resistance which is visible in the impedance spectra by the increase of both the real, resistive part and the imaginary, capacitive contribution. In this case the real part value, calculated by the difference between the low-frequency and high-frequency intersections of the real axis by the impedance spectrum, undergoes an increase to 0.743 Ωcm^2. The uneven current distribution over the cathode surface, due to a difference between the in-plane and cross-plane resistances (9) affects the electrode/current collector interface in a similar way to what happens in the electrode/electrolyte interface (10, 11). The result is the presence of cathodic sections where low or no current is flowing causing local inactivity of the electrode.

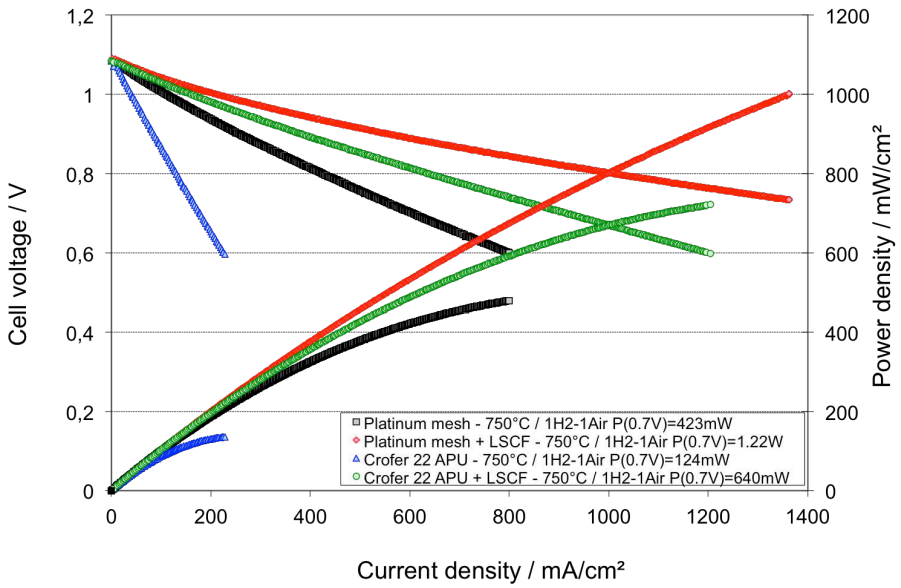

Figure 3. I-V curves and power densities of a cell measured at 750°C, 1 Nlpm air at the cathode side and 1 Nlpm H_2 with 3 vol.%. H_2O at the anode.

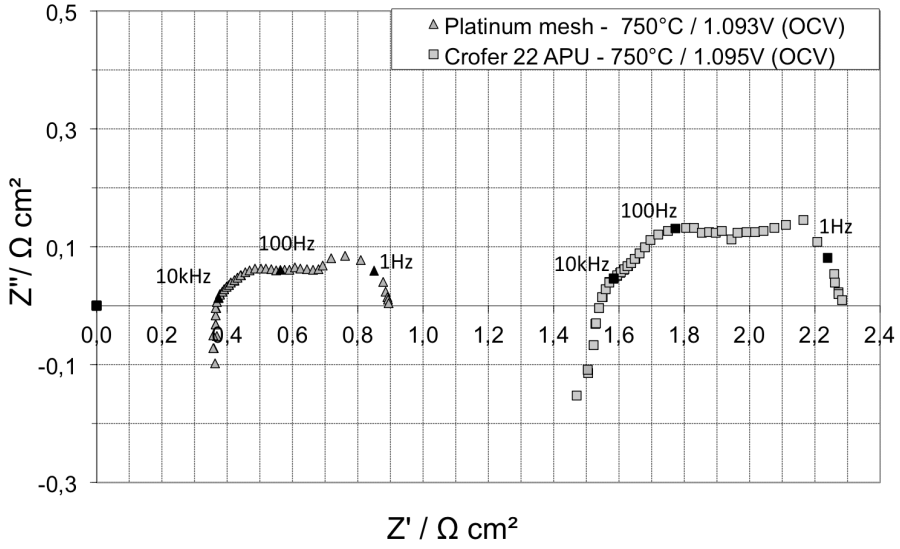

Figure 4. Impedance spectra of the cell contacted with platinum mesh and with Crofer 22 APU as cathodic current collector.

The application of a LSCF contacting paste layer between the cathode and the current collector resulted in a beneficial effect in case of both platinum mesh and bipolar plate solutions. In the first case it was not possible to investigate the power output for the whole range down to 0.6 V because of current limitations of the testing device to avoid problems regarding the wiring, however it has been calculated by an extrapolation from intermediate values of the I-V curve that the cell can reach a power output of 1.22Wcm^{-2} at 0.7 V corresponding to an improvement of 188% compared to the cell tested without contacting material. The cell polarization decreased by 11% reaching a value of 0.463 Ωcm^2.

The application of LSCF contacting paste between the cathode and the Crofer 22 APU bipolar plate led to intermediate performances between the before mentioned cells.

Figure 5 shows that the use of a contacting layer renders similarly the total cell ASR despite the differences in the current collector geometries. The use of Crofer 22 APU resulted in higher ohmic resistance, however, a lower polarization contribution in the same cell was measured that compensates the values. The comparison of such impedance results with the I-V curves highlights the role of the ohmic losses in the overall cell performances since even for similar total ASR values the power density is affected by contacting issues to a greater extent.

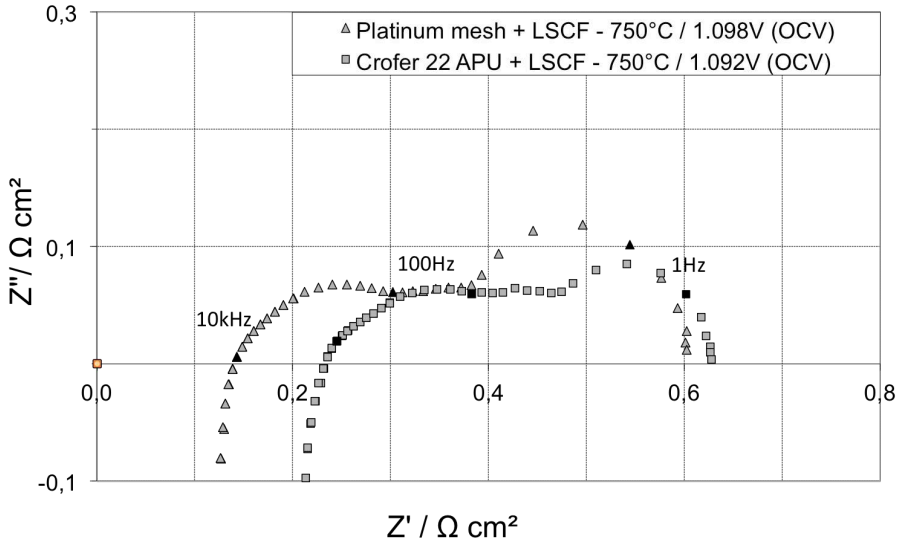

Figure 5. Impedance spectra of the cell contacted using a LSCF paste layer between the cathode and the current collector.

Degradation

The galvanostatic load applied on the cell contacted only with the platinum mesh resulted in a linear decrease of the cell voltage with a loss of 6 mV in 100 hours of test (figure 6). The curve is characterized by discontinuous steps in the potential values due to leakages in the sealing region. The application of the contacting paste layer led to similar behaviors with the loss of 3 mV in the case of platinum mesh as current collector and 6 mV for Crofer 22 APU. A different behavior has been observed in the degradation of the cell contacted directly with Crofer 22 APU where the voltage decrease was higher. In particular during the first hours of the experiment a fast degradation was measured that tended to be mitigated assuming a linear tendency after about 30 hours.

From the impedance measurements the increase of the cell polarization in the samples has been observed where the current collector has been applied in direct contact with the cathode. The contacting layer mitigated this effect as can be seen in the plot in figure 7. Changes of the ohmic contribution affected in a greater extent the cell directly contacted with the Crofer 22 APU bipolar plate where an increase of 77 mΩ was measured. No significant changes have been observed for the other contacting solutions.

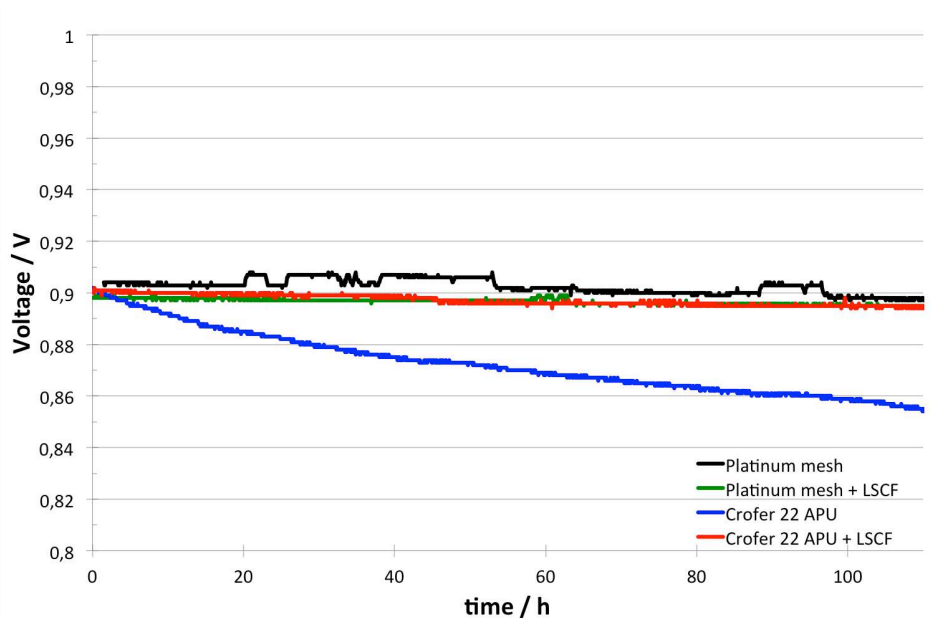

Figure 6. Evolution of the cell voltage during the galavanostatic load for all tested cells.

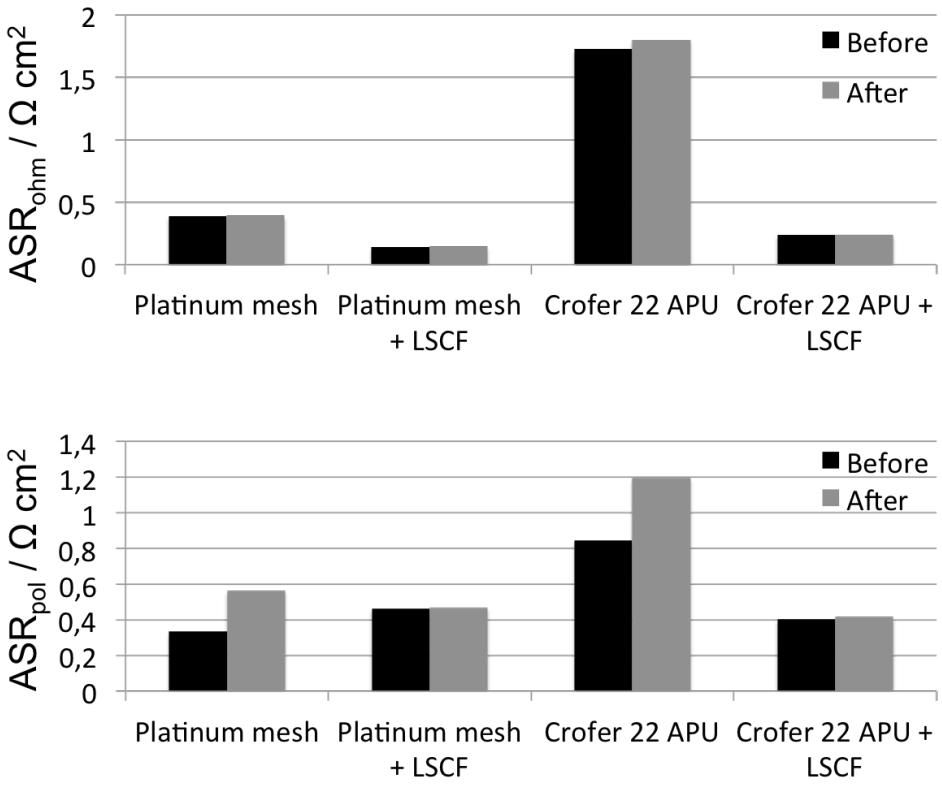

Figure 7. ASR of the ohmic (above) and polarization (below) contributions calculated from the impedance results.

TABLE I. Summary of the cell parameters before and after the galvanostatic test

Cell	Over-potential / mV		Power density / $mWcm^{-2}$		Current density / $mAcm^{-2}$
	before	after	before	after	
Platinum mesh	189	195	226	225	250
Platinum mesh + LSCF	200	203	506	504	563
Crofer 22 APU	193	236	70	67	78
Crofer 22 APU + LSCF	191	197	343	341	381

Post-experiment characterization

The post-experiment analyses revealed for all tested cells the presence of strontium at the interface between the electrolyte and the barrier layer (figure 8). Such phenomenon, that could be due to the porosity of the GDC layer, might be the cause of the lower performance measured compared to other state-of-the-art cells. The reactivity of strontium with the YSZ of the electrolyte causes the formation of low-conducting phases which are detrimental for the system performances (12).

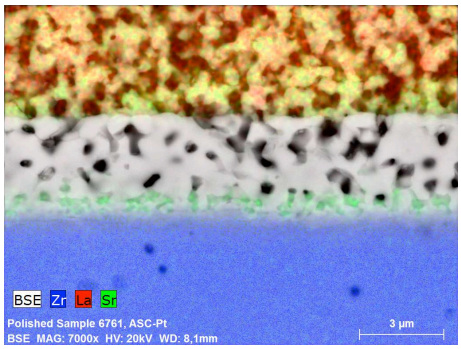

Figure 8. SEM-EDX map of the cross-section detail of the cathode/interlayer/electrolyte interfaces.

The cathodes showed inhomogeneous porosity in their section characterized by big pores far from the interlayer/cathode interface (figure 9). High irregularity has been found on top of the whole layer (figure 1) which could be responsible for lowered electrical contact with the current collector. The use of a contacting paste ensures a larger exploitation of the cathode surface for the current distribution as observed by the electrical measurements.

The steel as current collector on the cathode side promoted the pollution of the electrode as can be seen by the presence of chromium on the EDX map in figure 9. Such element is distributed along the whole electrode section with higher concentrations at the top of it in correspondence of the interface electrode/steel. EDX results have been confirmed by XRD analyses (figure 10) where the presence of new phases was identified in the cells tested with Crofer 22 APU bipolar plates. Also manganese and iron from the bipolar plate migrated together with chromium. The observed element migration, however, was not sufficient to observe significant changes in the electrode performances from the impedance investigations. The polarization ASR increase was more related to the absence of the contacting layer as shown in figure 7.

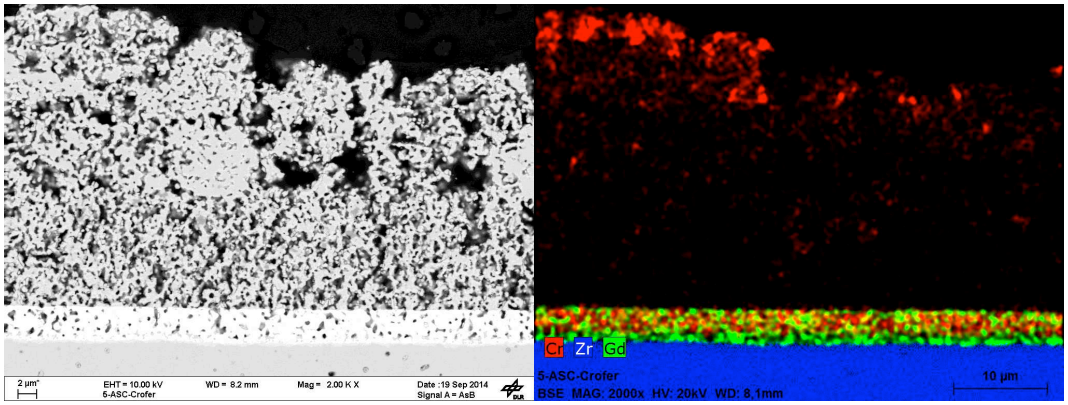

Figure 9. SEM-BSE image (left) and EDX map (right) of the cathode including the interlayer and part of the electrolyte.

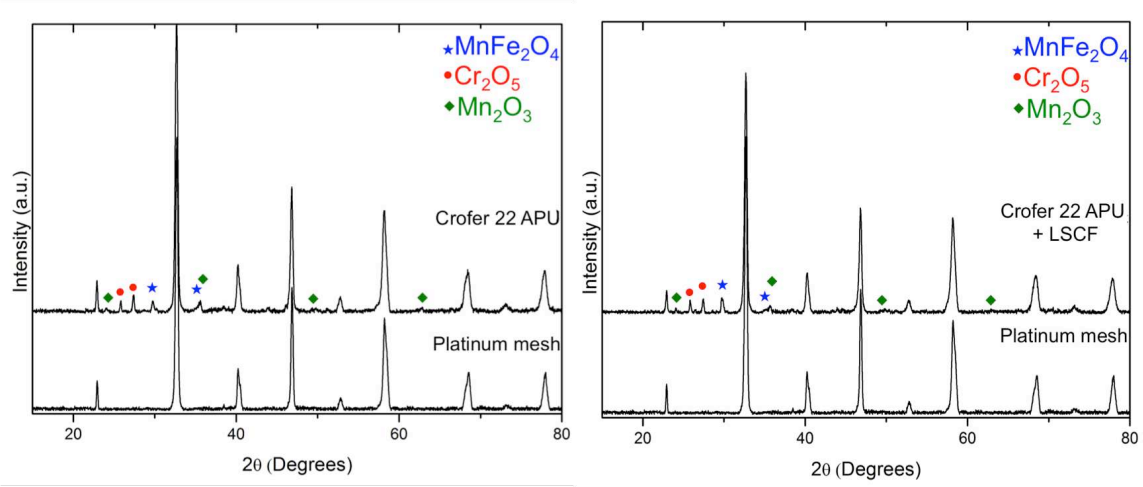

Figure 10. X-ray diffraction patterns of the cathode surface of the cell contacted with Crofer 22 APU current collector with (right) and without (left) contacting paste. The diffraction patterns are compared with those measured on the cell contacted only with platinum mesh at the cathode side.

Observing the bipolar plate in cross section (figure 11), a total coverage of the metal by an oxide scale with an average thickness of 2 µm can be seen where the current collector is in contact with the electrode (bipolar plate ribs). Such layer is mainly constituted of Fe, Cr and Mn as revealed by EDX analyses. The presence of Si and Ti in the whole oxide was also spotted with a decreasing amount through the scale section. A Cr-rich layer characterized by the presence of iron and manganese in solid solution has been found at the metal/oxide interface.

In correspondence of the channels, where the cathode gas flows during cell operation, the interconnect presents an oxide scale less dense than the previous one which, on the surface is characterized by larger crystals and porous structures. As can be seen from the EDX analyses the titanium concentration in the oxide is generally lower whereas the silicon amount is higher. The Ti beneath the steel surface is in this case higher. The observed oxide morphology made it difficult to properly distinguish the scale layers except the inner one, well adherent to the steel surface. It is reasonable to attribute the scale density and composition observed on the ribs to the effect of the current flow concentrated in such portion causing a local heating and a definite promotion of the alloy element migration. The morphological differences presented by the channel can be

related to the presence of flowing air, which subjects this location to higher oxygen partial pressures promoting a faster oxidation and chromium evaporation despite this area is characterized by the same electrical potential of the rib.

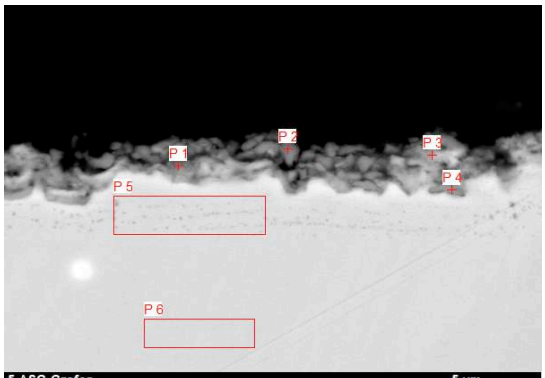

Spectrum	O	Al	Si	Cl	Ca	Ti	Cr	Mn	Fe
P 1	58,43	-	0,53	0,26	0,11	0,33	24,96	6,36	9,01
P 2	61,82	-	0,67	0,50	-	0,28	20,26	10,95	5,52
P 3	53,61	0,17	0,67	0,18	0,16	0,62	21,71	7,23	15,64
P 4	47,28	-	1,03	0,14	-	0,40	26,61	7,50	17,04
P 5	3,52	-	0,21	-	-	0,78	18,10	-	77,39
P 6	-	-	-	-	-	-	21,06	-	78,94

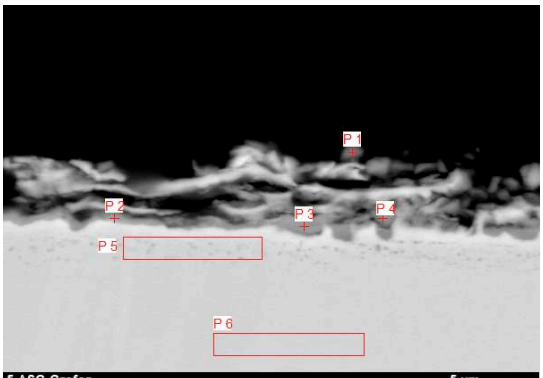

Spectrum	O	Al	Si	Cl	Ca	Ti	Cr	Mn	Fe
P 1	57,06	-	0,60	0,45	0,14	0,11	9,15	23,86	8,64
P 2	48,43	0,10	1,21	-	0,11	0,32	25,02	4,55	20,26
P 3	48,30	0,10	1,20	-	-	0,51	23,19	6,98	19,71
P 4	51,30	-	2,18	-	-	0,44	28,90	8,33	8,86
P 5	6,10	-	0,28	-	-	1,23	20,64	-	71,76
P 6	-	-	-	-	-	-	22,34	-	77,66

Figure 11. SEM-BSE image and EDX point analyses on cross-sections of the bipolar plates in correspondence of the rib (left) and the channel (right); the unit of the table of results is in at.%.

Conclusions

In this work anode-supported cells have been tested with different cathodic contacting solutions in terms of geometry and the application of a contacting paste layer between the electrode and the current collector. The measured cell performances by means of current-voltage curves and electrochemical impedance spectroscopy highlighted the influence of the contribution of the ohmic losses on the cell polarization and the direct effect on the power output reduction. The galvanostatic test of 100 hours caused an increase of the polarization ASR on the cell where the current collector was in contact directly with the cathode. The use of a contacting layer between the two components mitigated this effect enhancing the current distribution over the electrode surface resulting in a significant reduction the cell degradation. The application of Crofer 22 APU bipolar plate as current collector promoted the migration of Cr, Fe and Mn within the electrode causing the formation of additional phases which effect on the cell performances was not revealed by the electrochemical measurement in the testing time. However, visible differences in the oxide structure and composition between the ribs and channels were observed on the steel surface due to the diversity of the local conditions in terms of oxygen partial pressure, temperature and electrical current flow.

Acknowledgments

The authors would like to acknowledge I. Plock, G. Steinhilber and O. Freitag for the technical support.

References

1. S. P. Jiang, *J. Electrochem. Soc.*, 148(8), A887 (2001)
2. Z. Lu, J. Hardy, J. Templeton, J. Stevenson, *Journal of Power Sources,* 196, 39 (2011)
3. S.P. Jiang, J.G. Love, L. Apateanu, *Solid State Ionics*, 160, 15 (2003)
4. M. C. Tucker, L. Cheng, L.C. DeJonghe, *Journal of Power Sources*, 196, 8313 (2011)
5. V.A.C. Haanappel, N. Jordan, A. Mai, J. Mertens, J.M. Serra, F. Tietz, S. Uhlenbruck, I.C. Vinke, M.J. Smith, L.G.J. de Haart, *J. Fuel Cell Sci. Technol* 6(2), 021302 (2009)
6. V.A.C. Haanappel, A. Mai, J. Mertens, *Solid State Ionics,* 177, 2033 (2006)
7. V.A.C. Haanappel, M.J. Smith, *Journal of Power Sources*, 171, 169 (2007)
8. C. Comminges, Q.X. Fu, M. Zahid, N. Y. Steiner, O. Bucheli*, Electrochimica Acta,* 59, 367 (2012)
9. F.H. van Heuveln, H.J.M. Bouwmeester, F.P.F. van Berkel, *J. Electrochem. Soc.,*144, 126 (1997)
10. J.Fleig, J. Maier, *J. Electrochem. Soc*., 144, L302 (1997)
11. A. C. S. Sabioni, A. N. Huntz, F. Millot, C. Monty, *Philos. Mag. A*, 66, 361 (1992)
12. H.-G. Jung, Y.-K. Sun, H. Y. Jung, J.S. Park, H.-R. Kim, G.-H. Kim, H.-W. Lee, J.-H. Lee, *Solid State Ionics*, 179, 1535 (2008)